V. Summary and Conclusions

It has been demonstrated that nickel cluster ions, size-selected by quadrupole mass spectrometry, react with carbon monoxide to yield complexes of the type $Ni_n(CO)_k^+$ and $Ni_nC(CO)_l^+$ where n ranges from 1 through 13 and k and l correlate extremely well with the electron-counting rules proposed by Lauher (see Figure 6 and Table II).

The data presented here were obtained primarily for the purpose of identifying the products, but, as we have already shown for Ag_n^+ clusters,[27] there is a sufficient particle flux to carry out these reactions on a synthetic scale. One can readily envisage applications to surface chemistry and to catalysis, and these will be the subject of future reports.

Acknowledgment. We thank the Institute of Experimental Physics at the Swiss Federal Institute of Technology in Lausanne and the Swiss National Science Foundation for supporting this collaborative project.

Registry No. Ni_2^+, 51404-27-4; Ni_3^+, 51404-28-5; Ni_4^+, 73145-96-7; Ni_5^+, 73145-97-8; Ni_6^+, 73145-98-9; Ni_7^+, 73145-99-0; Ni_8^+, 73146-00-6; Ni_9^+, 106543-06-0; Ni_{10}^+, 106543-05-9; Ni_{11}^+, 106567-05-9; Ni_{12}^+, 106543-07-1; Ni_{13}^+, 106543-08-2; CO, 630-08-0.

---

(27) Fayet, P.; Granzer, F.; Hegenbart, G.; Moisar, E.; Pischel, B.; Wöste, L. *Phys. Rev. Lett.* **1985**, *55*, 3002.

Electron Self-Exchanges in an Osmium Polypyridine Redox Polymer in the Absence of Liquid Solvents by Solid-State Voltammetry

J. C. Jernigan and Royce W. Murray*

Contribution from the Kenan Laboratories of Chemistry, University of North Carolina, Chapel Hill, North Carolina 27514. *Received August 18, 1986*

Abstract: This paper describes voltammetry in the absence of external liquid electrolytes of films of the redox polymer poly$[Os(bpy)_2(vpy)_2](X)_n$ sandwiched between Pt and porous Au electrodes and bathed in acetonitrile vapor, dry N_2, 10^{-6} torr vacuum, toluene liquid, or toluene vapor. The voltammetry differs for $n = 1$, 2, or 2.5 and is quantitatively explained with theory based on electron diffusion in the polymer occurring by electron self-exchange reactions between polymer sites. Electron diffusion coefficients, D_e, depend strongly on the bathing medium, being the same in acetonitrile vapor and liquid for the poly[Os(III/II)] and poly[Os(II/I)] couples, but depressed for the former and elevated for the latter in films contacted only by dry N_2. The latter circumstance yields the largest electron diffusion coefficient measured thus far for a localized electronic state redox polymer, 1.7×10^{-6} cm^2/s.

Learning how to conduct quantitatively interpretable voltammetry of electrochemical reactions in the absence of liquid solvents may lead to discoveries of new chemical sensors, applications in energy storage and in macromolecular electronics, and how the kinetics and thermodynamics of electron-transfer reactions respond to solvation. Most previous solid-state electrochemical investigations[1] have focused on energy storage applications and consequently a limited range of redox couples (Li, Na), in cells fashioned from ionically conductive inorganic lattice and layer compounds. Recent applications of ionically conducting polymers[2] are, on the other hand, expanding the range of solid-state electrochemical phenomena studied, to include photoelectrochemical[3] and electrochromic[4] cells, solid-state polymer batteries,[5] an in situ UHV electron spectroscopy experiment,[6] a gas detector,[7] and electron transport in redox polymers.[8] An additional point of note is how the electron transfer chemistry of solid-state materials can yield insights into the internal dynamics of solid materials as illustrated by recent work by Hendrickson et al.[9]

In this paper, we explore how the rates of the electron self-exchange reactions between Os(III) and Os(II), and between Os(II) and Os(I), complex sites in films of the polymer[10] poly$[Os(bpy)_2(vpy)_2](X)_2$, depend upon the medium bathing the polymer film: a liquid solvent, a solvent vapor, a dry gas, or vacuum. To measure these rates, we use sandwich electrode microstructures[11] containing ca. 80–800-nm films of the poly$[Os(bpy)_2(vpy)_2](X)_2$ polymer. The steady-state currents which flow between the two metal contacts of the sandwich microstructure when their potentials are set so as to oxidize and reduce, respectively, osmium sites at the opposing metal/polymer interfaces (schematically shown in Figure 1, top) are controlled by electron self-exchanges between oxidized and reduced sites in the intervening polymer film. The rate of these self-exchanges is measured

---

(1) (a) Linford, R. G.; Hackwood, S. *Chem. Rev.* **1981**, *81*, 327 and references therein. (b) Raleigh, D. O. In *Electroanalytical Chemistry*; Bard, A. J., Ed.; Marcel Dekker: New York, 1973; Vol. 6.

(2) (a) Armand, M. B.; Chabagno, J. M.; Duclot, M. J. *Fast Ion Transport in Solids*; Vashishta, P., Ed.; North Holland: New York, 1979; pp 131. (b) Armand, M. B. *Solid State Ionics* **1983**, *9/10*, 745. (c) Spindler, R.; Shriver, D. F. *Macromolecules* **1986**, *19*, 347. (d) Dupon, R.; Papke, B. L.; Ratner, M. A.; Shriver, D. F. *J. Electrochem. Soc.* **1984**, *131*, 586. (e) Hardy, L. C.; Shriver, D. F. *J. Am. Chem. Soc.* **1985**, *107*, 3823. (f) Reitman, E. A.; Kaplan, M. L.; Cava, R. J. *Solid State Ionics* **1985**, *17*, 67.

(3) (a) Inganas, O.; Skotheim, T. A. *Mol. Cryst. Liq. Cryst.* **1985**, *121*, 285. (b) Inganas, O.; Skotheim, T. A.; Feldberg, S. W. *Solid State Ionics* **1986**, *18/19*, 332.

(4) Calvert, J. M.; Manuccia, T. J.; Nowak, R. J. *J. Electrochem. Soc.* **1986**, *133*, 951.

(5) (a) Schoonan, J.; Wolfert, A.; Untereker, D. F. *Solid State Ionics* **1983**, *11*, 187. (b) Matsumoto, T.; Matsunaga, K. *Bull. Chem. Soc. Jpn.* **1981**, *54*, 648. (c) Chiang, C. K. *Polymer* **1981**, *22*, 1454.

(6) (a) Skotheim, T. A.; Florit, M. I.; Melo, A.; O'Grady, W. E. *Mol. Cryst. Liq. Cryst.* **1985**, *121*, 291. (b) Skotheim, T. A.; Florit, M. I.; Melo, A.; O'Grady, W. E. *Phys. Rev. B* **1984**, *30*, 4846.

(7) (a) Pons, S.; Daschbach, J.; Fleischmann, M. 191st National Meeting of the American Chemical Society, New York, NY, 1986; ANAL 103. (b) Pons, S. ONR-NSF Workshop on Ultramicroelectrodes; Homestead, Utah, Jan 1986.

(8) Jernigan, J. C.; Chidsey, C. E. D.; Murray, R. W. *J. Am. Chem. Soc.* **1985**, *107*, 2824.

(9) (a) Lambert, Susan L.; Spiro, C. L.; Gagne, R. R.; Hendrickson, N. *Inorg. Chem.* **1982**, *21*, 68–72. (b) Mabad, B.; Cassoux, P.; Tuchagues, J. P.; Hendrickson, D. N. *Ibid.* **1986**, *25*, 1420. (c) Mabad, B.; Tuchagues, Y.; Hendrickson, D. N. *J. Am. Chem. Soc.* **1985**, *107*, 2801.

(10) (a) Calvert, J. M.; Schmehl, R. H.; Sullivan, B. P.; Facci, J. S.; Meyer, T. J.; Murray, R. W. *Inorg. Chem.* **1983**, *22*, 2151. (b) bpy is 2,2′-bipyridine and vpy is 4-vinylpyridine.

(11) (a) Pickup, P. G.; Murray, R. W. *J. Am. Chem. Soc.* **1983**, *105*, 4510. (b) Pickup, P. G.; Murray, R. W. *J. Electrochem. Soc.* **1984**, *131*, 833. (c) Pickup, P. G.; Kutner, W.; Leidner, C. R.; Murray, R. W. *J. Am. Chem. Soc.* **1984**, *106*, 1991.

0002-7863/87/1509-1738$01.50/0

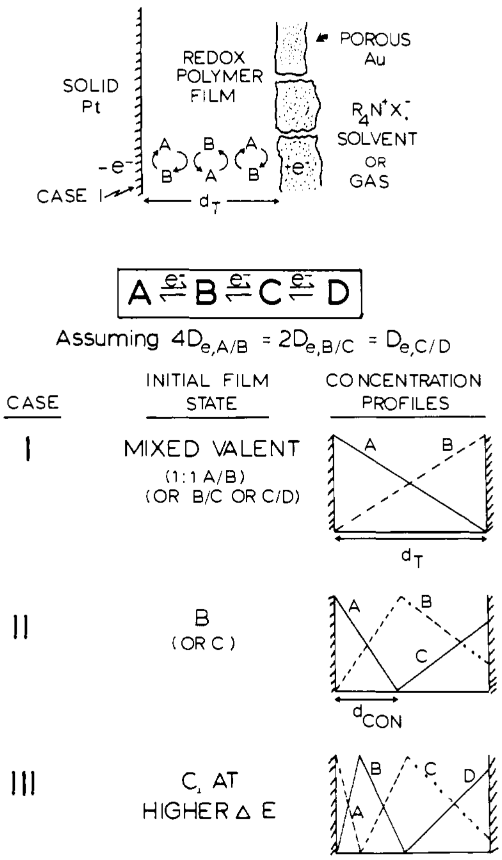

Figure 1. Sandwich electrode cross section (top) and concentration profiles of polymer sites A, B, C, D for cases I-III under conditions of limiting current flow.

in terms of the electron diffusion coefficient, D_e (cm^2/s).

The situations which are most novel for electron self-exchanges are those where no liquid or external electrolyte contacts the polymer film. In such cases, electroneutrality constraints ("ion budgeting")[8] cause the observable solid-state voltammetry to depend on the initial average oxidation state of the film. The film[12] can be initially (case I) 1:1 mixed-valent poly[Os(III/II)], (case II) all in the poly[Os(II)] state, or (case III) all in the poly[Os(I)] state. Electron diffusion (hopping) theory[13] is used to quantitatively interpret currents of the observed case I–III voltammograms and to extract values of D_e for the poly[Os(III/II)] and poly[Os(II/I)] couples. Since D_e is thought to be proportional[11c,14] to the self-exchange rate constant, $k_{ex,app}$, we are able in this way to measure how the self-exchange rates for these couples respond to whether the sandwiched polymer film is bathed (via the porous Au electrode side) in dry N$_2$, air, CH$_3$CN vapor, vacuum, toluene liquid or vapor, or heptane vapor.

Information about how the formal potentials of pairs of osmium redox couples vary according to the bathing medium is also derived from the case II and III voltammograms. We have further observed that the polymer films respond quite rapidly to transient changes in the bathing gas, and that the electron diffusion rate can vary according to whether the mobile, charge compensating counterion X$^-$ is ClO$_4^-$ or tosylate (p-CH$_3$C$_6$H$_4$SO$_3^-$, Tos$^-$).

Experimental Section

Electrodes and Apparatus. The glass-shrouded Pt microdisk electrodes (area = 0.0032 or 0.00197 cm^2), the electropolymerization of poly[Os(bpy)$_2$(vpy)$_2$](X)$_2$ films onto the Pt, and the vapor deposition of a thin, porous Au electrode on top of the polymer and overlapping (for electrical contact) onto an adjacent Pt microdisk, were as described previously.[11c] Potentials of the Pt and Au electrodes were controlled using Pine Instrument Co. (Grove City, PA) Model RDE 3 and RDE 4 bipotentiostats.

Chemicals. Acetonitrile (Burdick and Jackson UV Spectra quality) was stored over 4-Å molecular sieves. Toluene (Fisher, ACS grade) was refluxed several hours over CaH$_2$ and similarly stored. Et$_4$NClO$_4$ and Hx$_4$NClO$_4$ electrolytes were recrystallized three times from water and ethyl acetate, respectively, and vacuum oven dried. Et$_4$NTos (Alfa, 98%) was recrystallized twice from ethyl acetate.

Experimental Procedures. Following electropolymerization, the polymer is in the poly[Os(II)(bpy)$_2$(vpy)$_2$](ClO$_4$)$_2$ state, and during the course of the Au evaporation becomes thoroughly dried in vacuo. For (case II) voltammetry of films in the poly[Os(II)] state, the sandwich is exposed to no further liquids prior to taking solid-state voltammograms. When a given sandwich electrode is successively exposed to different bathing gases, the voltammograms were taken in the order of least to most polar gas constituent (i.e., N$_2$, vacuum, heptane, toluene vapors before CH$_3$CN vapor), calculated to minimize carryover of adsorbed gas constituents.

For case I voltammetry (films in the 1:1 poly[Os(III/II)] state), poly[Os(bpy)$_2$(vpy)$_2$](ClO$_4$)$_2$ sandwiches are immersed in Et$_4$NClO$_4$/CH$_3$CN electrolyte solution and the Pt electrode potentiostated at the $E^{\circ\prime}$ for the Os(III/II) couple in the film until the current dies to background (a few seconds). The electrochemical control is then disconnected and the mixed-valent electrode raised from the solution, rinsed with pure acetonitrile, and allowed to dry at ambient temperature. Preparation of poly[Os(I)(bpy)$_2$(vpy)$_2$](ClO$_4$) films (case III) was done similarly, except in a Vacuum Atmospheres glovebox, since such films are O$_2$ sensitive.

Solid-state voltammetry experiments involve simply scanning a ΔE applied between the Pt (normally the + terminal) and Au electrodes of the sandwich. Following the solid-state voltammetry, postmortem cyclic voltammetry is conducted by placing the sandwich in Et$_4$NClO$_4$/CH$_3$CN electrolyte solution, leaving the Au electrode disconnected, and scanning the Pt electrode potential, relative to a SSCE, to ascertain that the amount of electroactive Os(III/II) had not changed from that originally deposited by electropolymerization. At that time, values of the electron diffusion coefficient, D_e^l, for that sandwich electrode in contact with electrolyte solution were also taken by controlling the potentials of *both* the Pt and Au electrodes relative to a SSCE as described previously.[11c]

Finally, some comments are in order on the experimental uncertainty of the D_e values reported below in Table I. There is a substantial variability of D_e values, often up to a factor of 2×, obtained from repeated preparations of a given type of sandwich electrode. The reader will note that we are accordingly careful not to attempt interpretations of differences of this magnitude in D_e values among bathing media. Exceptions lie in cases (of Figures 4 and 6) where a given sandwich electrode is switched among bathing media; such relative responses are much more reliable in revealing medium effects.

Theory for Solid-State Voltammetry of Redox Polymer Sandwiches

The following theory is generalized to any redox polymer film whose electron conductivity depends upon self-exchange reactions driven solely by concentration gradients of oxidized and reduced species and hence is describable[11c,13-15] by Fick's first law and an electron diffusion coefficient D_e. Electron diffusion coefficients measured in the absence and presence of liquids will be labeled D_e^g and D_e^l, respectively. A hypothetical redox polymer with three, widely spaced, reversible redox couples is assumed, A/B, B/C, and C/D, corresponding to the poly[Os(III/II)], poly[Os(II/I)], and poly[Os(I/0)] couples in our films. We assume that D_e is larger for the more reduced couples, although this is not essential to formulate a theory. In applying Fick's law, it is also assumed that the film is sufficiently thick (that there are a sufficient number of monolayers of redox sites) within a given concentration gradient interval to satisfy basic continuity-of-medium requirements. Also, the small enhancements of D_e that will arise due to coupling

---

[12] Abbreviations: poly[Os(III/II)] is poly[Os(III/II)(bpy)$_2$(vpy)$_2$](X)$_{2.5}$; poly[Os(II)] is poly[Os(II)(bpy)$_2$(vpy)](X)$_2$; poly[Os(I)] is poly[Os(I)(bpy)$_2$(vpy)$_2$]X.

[13] (a) Oyama, N.; Anson, F. C. *J. Electrochem. Soc.* **1980**, *127*, 640. (b) Daum, P.; Lenhard, J. R.; Rolison, D.; Murray, R. W. *J. Am. Chem. Soc.* **1980**, *102*, 4649. (c) Kaufman, F. B.; Schroeder, A. H.; Engler, E. M.; Kramer, S. R.; Chambers, J. Q. *Ibid.* **1980**, *102*, 483. (d) Nowak, R. J.; Schultz, F. A.; Umana, M.; Lam, R.; Murray, R. W. *Anal. Chem.* **1980**, *52*, 315. (e) Kaufman, F. B.; Engler, E. M. *J. Am. Chem. Soc.* **1979**, *101*, 547.

[14] (a) Andrieux, C. P.; Saveant, J.-M. *J. Electroanal. Chem.* **1980**, *111*, 377. (b) Laviron, E. *Ibid.* **1980**, *112*, 1.

[15] The theory also applies with minor differences to two terminal array electrodes: (a) Chidsey, C. E. D.; Feldman, B. J.; Lundgren, C.; Murray, R. W. *Anal. Chem.* **1986**, *58*, 601. (b) Kittlesen, G. P.; White, H. S.; Wrighton, M. S. *J. Am. Chem. Soc.* **1984**, *106*, 7389. (c) Bard, A. J.; Crayston, J. A.; Kittelsen, G. P.; Shea, T. V.; Wrighton, M. S. *Anal. Chem.* **1986**, *58*, 2321.

Table I. Electron Diffusion Coefficients for Poly$[Os(bpy)_2(vpy)_2](ClO_4)_2$ Redox Couples Measured in Various Environments

bathing gases[a]	$\Gamma_T \times 10^8$, mol/cm^2 [b]	$D_e \times 10^8$, cm^2/s $D^g_{e,3/2}$ (no.)[c]	 $D^g_{e,2/1}$	 $D^g_{e,1/0}$	rel D_e 3/2:2/1:1/0
CH_3CN vapor[d]	1.4 to 3.0	0.9 ± 0.4 (6)	14 ± 8	149	1:15:165
toluene vapor[d]	3.0	0.25 ± 0.02 (2)	166 ± 19		1:664:na
room air	3.0	0.41 ± 0.09 (2)			
dry N_2	1.4 to 2.0	0.4 ± 0.2 (2)	120 ± 47		1:300:na
liquid/electrolyte[e]	$\Gamma_T \times 10^8$, mol/cm^2 [b]	$D^l_{e,3/2}$ no.[c]	$D^l_{e,2/1}$	$D^l_{e,1/0}$	
0.1 M Et_4NClO_4/CH_3CN	0.7 to 7	1.2 ± 0.5 (17)	5.9 ± 1.8 (16)	96 ± 16 (6)	1:5:79
		0.8 ± 0.3[f] (14)	2.4 ± 0.9[f] (8)	20 ± 7[f] (12)	1:3:25
0.2 M Hx_4NClO_4/toluene	0.6 to 2	0.35 ± 0.08 (3)	0.48 ± 0.37 (3)	18 ± 7 (3)	1:1.4:51
		0.10[g]			
0.1 M Et_4NTos/CH_3CN	2 to 4	0.15 ± 0.05 (3)	0.64 ± 0.4 (3)		1:4:na

[a] Case I: $D^g_{e,3/2}$ evaluated using mixed-valent poly$[Os(III/II)(bpy)_2(vpy)_2](ClO_4)_2$ films prepared by electrolysis at 0.73 V vs. SSCE in 0.1 M Et_4NClO_4/CH_3CN, followed by rinsing with pure CH_3CN and drying. $D^g_{e,2/1}$ and $D^g_{e,1/0}$ deduced from analysis of disproportionation voltammograms using $D^g_{e,3/2}$ values and eq 2 and 5. [b] Range of film coverages employed in D_e evaluations. [c] Number of trials. [d] Dry N_2 stream saturated (using bubbler) with vapor of liquid at room temperature. [e] Four electrode experiment, immersed in indicated liquid, where potentials of both Au and Pt controlled vs. SSCE (or in the case of toluene, a Ag wire), as described in ref 11. [f] From Table II, ref 11c. [g] From ref 20.

between electron diffusion and migration terms[16] are neglected in the formulation given here. Finally, since no external electrolyte is available, the electrochemical processes are constrained[8] by the "ion budget" of resident, mobile ClO_4^- ions within the film. This last point is a distinctive aspect of solid-state voltammetry. While we believe little if any excess electrolyte (e.g., $Et_4N^+ClO_4^-$) ions remain trapped in the film following its preparation,[17] the electroneutrality constraints of theory are still valid in their presence.

Three voltammetric situations prevail, depending on whether the hypothetical polymer is initially present (Figure 1) as: case I, mixed-valent state A/B (alternatively B/C or C/D); case II, oxidation state B (alternatively C); or case III, a second wave seen when starting with oxidation state C.

Case I, where both members of a reversible redox couple are initially present as in an A/B film, is the simplest. Application of any nonzero value of ΔE across the A/B sandwich causes A to be reduced at the negative electrode and B to be oxidized at the positive one. Since the ionic charges of A and B are different, resident counterions migrate from one side of the film to the other to maintain electroneutrality. Allowing at each ΔE a sufficient time to achieve steady state should give a sigmoidal, Nernstian-shaped voltammogram, symmetrical about $\Delta E = 0$ V, and with limiting currents representing complete concentration–polarization of A and B sites in the polymer[11] (see concentration profile diagram in Figure 1) and given by Fick's law,

$$i_{L,A/B} = nFAD^g_{e,A/B}C/d_T \tag{1}$$

where C is the smaller (accounting for the ion budget) of the two initial concentrations C_A and C_B, d_T is the film thickness, and $D^g_{e,A/B}$ represents electron diffusion by self-exchange between A and B sites. The limiting current given by eq 1 is maximized, $i_{L,A/B,max}$, when $C_A = C_B = 0.5C_T$ where C_T is the total site concentration.

In case II, where the film is initially all in oxidation state B, no current flows until the applied ΔE is sufficiently great to drive the disproportionation of B, oxidizing it to A at one electrode and reducing to C at the other. The $E_{1/2}$ of the resulting 2B → A + C voltammogram occurs at the difference, $\Delta E = E^{\circ\prime}(A/B) - E^{\circ\prime}(C/D)$, of the solid-state formal potentials of the A/B and B/C couples. Derivation of the voltammetric limiting current $i_{L,A/C}$ includes a statement of charge conservation and assumptions that the conproportionation that occurs between A and C in the interior of the film is complete and that, at the conproportionation plane (distance d_{con}), the electron fluxes $D^g_{e,A/B}[\delta[A]/\delta x]$ and $D^g_{e,B/C}[\delta[C]/\delta x]$ are equal:

$$i_{L,A/C} = [nFAD^g_{e,A/B}C_T/d_T]\{1 + [D^g_{e,B/C}/D^g_{e,A/B}]^{1/2}\} \tag{2}$$

$$i_{L,A/C}/i_{L,A/B,max} = 1 + [D^g_{e,B/C}/D^g_{e,A/B}]^{1/2} \tag{2a}$$

$$d_{con} = d_T[1 + (D^g_{e,B/C}/D^g_{e,A/B})^{1/2}]^{-1} \tag{3}$$

where the electron diffusion coefficients $D^g_{e,B/C}$ and $D^g_{e,A/B}$ describe electron self-exchanges between B and C and between A and B, respectively.[18] At $i_{L,A/C}$, as illustrated in Figure 1 for the situation $2D^g_{e,A/B} = D^g_{e,B/C}$, the more slowly electron exchanging redox couple is completely concentration-polarized, but the B/C couple is not, since charge conservation requires that the amounts of A and C generated be equal.[19]

When the film is initially in oxidation state C, two voltammetric waves are observed. The first wave is again a case II process and occurs when the applied ΔE suffices to drive the disproportionation reaction 2C → B + D. The voltammetric $E_{1/2}$ occurs at $\Delta E = E^{\circ\prime}(B/C) - E^{\circ\prime}(C/D)$, and the limiting current is

$$i_{L,B/D} = [nFAD^g_{e,B/C}C_T/d_T]\{1 + [D^g_{e,C/D}/D^g_{e,B/C}]^{1/2}\} \tag{4}$$

$$i_{L,B/D}/i_{L,B/C,max} = 1 + [D^g_{e,C/D}/D^g_{e,B/C}]^{1/2} \tag{4a}$$

The second wave is the case III process (Figure 1), where B is further oxidized to A at the positive electrode in an overall disproportionation cell reaction 3C → A + 2D. $E_{1/2}$ occurs at $\Delta E = E^{\circ\prime}(A/B) - E^{\circ\prime}(C/D)$. Derivation of the limiting current for case III involves assumed completeness of now two conproportionation reactions occurring in the interior of the film (between A and C and between B and D), and gives

$$i_{L,A/D} = [nFAD^g_{e,A/B}C_T/d_T] \times \{1 + D^g_{e,B/C}/D^g_{e,A/B} + [(D^g_{e,C/D}/D^g_{e,A/B})(1 + D^g_{e,B/C}/D^g_{e,A/B})]^{1/2}\} \tag{5}$$

$$i_{L,A/D}/i_{L,A/B,max} = 1 + D^g_{e,B/C}/D^g_{e,A/B} + [(D^g_{e,C/D}/D^g_{e,A/B})(1 + D^g_{e,B/C}/D^g_{e,A/B})]^{1/2} \tag{5a}$$

where all three electron diffusion coefficients now appear. A

---

(16) (a) The coupling of migration and electron diffusion terms as recently formulated by Buck[16b] is predicted to elevate the apparent D_e by ca. 22% for a Pt/poly[Os(II/III)]/Au sandwich in contact with liquid electrolyte; the effect is 44% for a Pt/poly[Os(I/II)]/Au sandwich. These factors are within the experimental uncertainties of the present measurements (see Experimental Section). (b) Buck, R. P., submitted for publication.

(17) The concentration of cationic charges and ClO_4^- ions in the poly$[Os(bpy)_2(vpy)_2](ClO_4)_2$ polymer exceeds 2 M. Consequently, Donnan exclusion should force the internal concentration of any intruding $Et_4N^+ClO_4^-$ electrolyte to low values, especially during the copious rinsing with pure acetonitrile solvent, containing no electrolyte, that follows adjustment of the film's oxidation state.

(18) Equations 2a, 4a, and 5a are simplified forms where $i_{L,A/B,max}$, the limiting current in a case I film with a 1:1 mixed-valent A/B composition is substituted for the first right-hand-side term of eq 2 and 5, and where $i_{L,B/C,max}$, the limiting current in a case I film with a 1:1 mixed-valent B/C composition, is similarly substituted in eq 4.

(19) The reason that no case III voltammetric wave occurs for a film initially in the B state, even at potentials thermodynamically permitting a 3B → 2A + D reaction, is that the A gradient is completely concentration polarized and incapable of accepting the additional counterions derived from further reduction of C to D. It is also useful to note that films initially in the A and D states should exhibit no voltammetry at all.

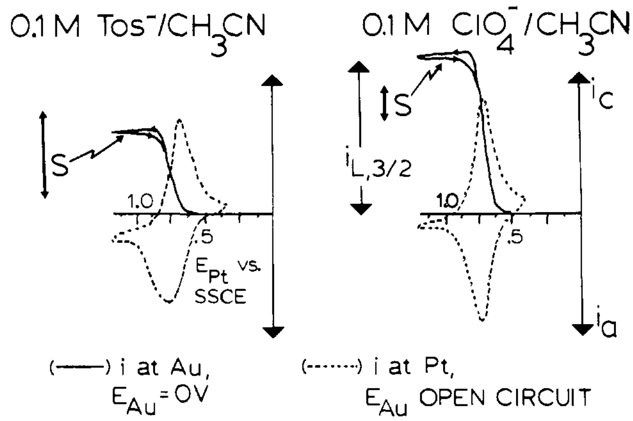

Figure 2. Voltammetry of the same 3.8 × 10^{-8} mol/cm^2 Pt/poly[Os(bpy)$_2$(vpy)$_2$]$^{2+}$/Au sandwich in two different liquid electrolyte solutions. E_{Pt} is swept, the Au electrode potential is controlled at 0 V to produce the steady-state sandwich voltammograms (—) and E_{Au} is open circuit to produce the cyclic voltammograms (---). Scan rates 5 mV/s (—) and 50 mV/s (---). S = 15.6 mA/cm^2; note difference in sensitivity scale for the two steady-state voltammograms (—).

diagram of the concentration profiles for this case (Figure 1) shows that the profile of the most slowly diffusing redox couple, A/B, is completely polarized, that of the B/C couple is also polarized owing to the complete conproportionation reactions, while that of the C/D couple is far from polarized owing to charge conservation constraints.

Results and Discussion

Electron Diffusion in Pt/Poly[Os(bpy)$_2$(vpy)$_2$](X)$_n$/Au Sandwiches Immersed in Liquid Solvents Containing Electrolytes. Because we wanted to compare electron mobilities in films immersed in liquids (D_e^l) with those bathed in gases (D_e^g), previous measurements[11,20] of D_e^l values were extended in the present study. Figure 2 contains example voltammograms.[21] Results for $D_{e,3/2}^l$, $D_{e,2/1}^l$ and $D_{e,1/0}^l$, for the poly[Os(II/III)], poly[Os(I/II)], and poly[Os(I/0)] couples, respectively, in Et$_4$NClO$_4$/CH$_3$CN liquid electrolyte solutions (Table I, lower part) agree with previous available data[11c] within a factor of about 2 (a common variability of D_e^l measurements). Table I includes data in Hx$_4$NClO$_4$/toluene; note that the self-exchange rates are all depressed in this low dielectric medium as compared to acetonitrile. $D_{e,3/2}^l$ and $D_{e,2/1}^l$ self-exchanges are also depressed[22] by use of the more bulky tosylate anion as the charge compensating anion of the osmium polymer instead of perchlorate; compare the $i_{L,3/2}$ limiting currents in Figure 2A,B.

Case I. Electron Diffusion in Mixed-Valent Pt/Poly[Os(III/II)(bpy)$_2$(vpy)$_2$](ClO$_4$)$_{2.5}$/Au Sandwiches in Various Bathing Gases. Sandwiches containing 1:1 mixtures of the poly[Os(II)] and poly[Os(III)] oxidation states were prepared by electrolysis of films at $E°'$ in 0.1 M Et$_4$NClO$_4$/CH$_3$CN followed by rinsing and air-drying (Figure 3). Upon bathing a Pt/poly[Os(III/II)(bpy)$_2$(vpy)$_2$](ClO$_4$)$_{2.5}$/Au sandwich in acetonitrile vapor-saturated N$_2$, a symmetrical, sigmoidally shaped wave centered about zero (Figure 3A) results as the potential ΔE between the Pt and Au electrodes is varied. When $\Delta E = E_{\text{Pt}} - E_{\text{Au}}$ is positive, an anodic current flows at Pt, meaning that poly[Os(II)] is being oxidized there, with poly[Os(III)] being reduced at Au. These are all characteristics expected for the mixed-valent case I. At the limiting current, the poly[Os(II)] and poly[Os(III)] sites have concentrations distributed as shown for case I in Figure 1 and ClO$_4^-$ ions have migrated to the poly[Os(III)] side. For electroneutrality reasons, no further voltammetric features are observed (Figure 3B) out to ΔE = 3 V.

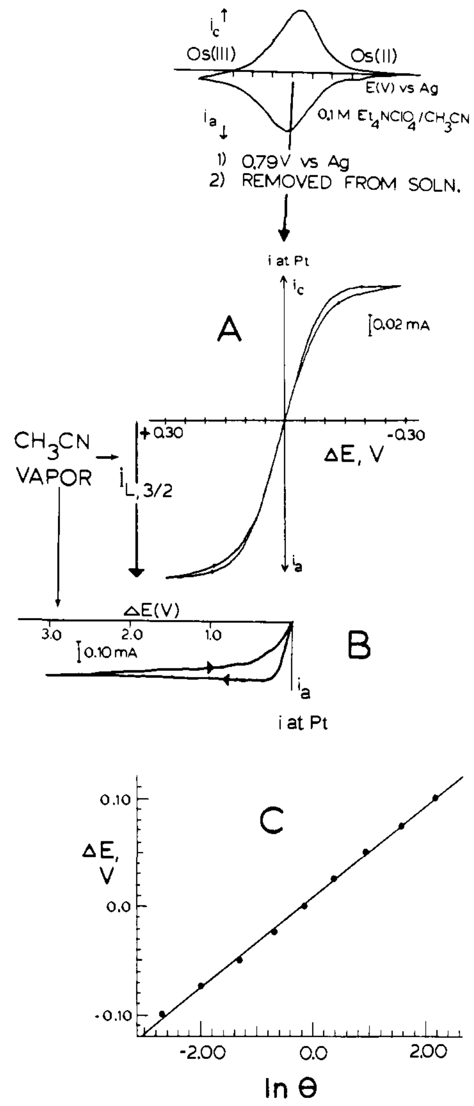

Figure 3. Case I experiments in CH$_3$CN vapor with 1:1 Os(III/II) sandwiches, Pt/poly[Os(III/II)(bpy)$_2$(vpy)$_2$](ClO$_4$)$_{2.5}$/Au, prepared by electrolysis in liquid electrolyte (top) and transfer to vapor. Curves A and B are ΔE scans for different sandwiches (2.4 × 10^{-8} and 7.6 × 10^{-8} mol/cm^2, respectively) over different potential ranges at 5 mV/s. Curve C is a reversibility plot for voltammogram of curve A where $\theta = (i_{L,c} - i)/(i - i_{L,a})$.

Applying eq 1 to the limiting current $i_{L,3/2}$ of a number of voltammograms like Figure 3A produces (Table I, upper part) an average $D_{e,3/2}^g = 0.9 \times 10^{-8}$ cm^2/s in acetonitrile vapor. This is within experimental uncertainty indistinguishable from that observed ($D_{e,3/2}^l = 1.2 \times 10^{-8}$ cm^2/s) for the poly[Os(II/III)] couple in liquid acetonitrile. That is, lowering a Pt/poly[Os(III/II)(bpy)$_2$(vpy)$_2$](ClO$_4$)$_{2.5}$/Au sandwich through which a limiting current is already flowing (a sufficient ΔE being applied) from an acetonitrile vapor bath into a liquid Et$_4$NClO$_4$/CH$_3$CN solution would produce little or no change in the current flowing.

The shape of the solid-state voltammogram of Figure 3A, when analyzed according to the relationship for a reversible couple, gives a linear plot (Figure 3C) with 0.0429-V slope. An analogous comparison for the Figure 2 liquid electrolyte voltammogram gives a slope of 0.0279 V. The difference in slope means that the reversible current–potential wave is broader (on the potential axis)

---

[20] Geng, L.; Ewing, A. G.; Jernigan, J. C.; Murray, R. W. *Anal. Chem.* **1986**, *58*, 852.

[21] D_e^l for films contacted by liquid/electrolyte solutions is measured[11c] by adjusting the Au and Pt electrode potentials of a Pt/poly[Os(II)](X)$_2$/Au polymer sandwich, relative to a SSCE reference electrode, so as to oxidize and reduce opposing sides of the polymer film. For example, application of E_{Au} = 0 V vs. SSCE and scanning E_{Pt} positively as in Figure 2A should produce poly[Os(II)] and poly[Os(III)] concentration gradients exactly like those depicted for case I (Figure 1), and a limiting current $i_{L,3/2} = nFAD_{e,3/2}^lC_T/d_T$ where $D_{e,3/2}^l$ measures electron conduction via poly[Os(II)] sites self-exchanging with poly[Os(III)] sites in a liquid-bathed film.[11c]

[22] The cyclic voltammetric oxidation wave for the poly[Os(III/II)] couple is also broadened (Figure 2B) relative to the reduction wave, signifying appreciable, nonequilibrium site interaction effects when the film is made to accept the bulkier tosylate anion.

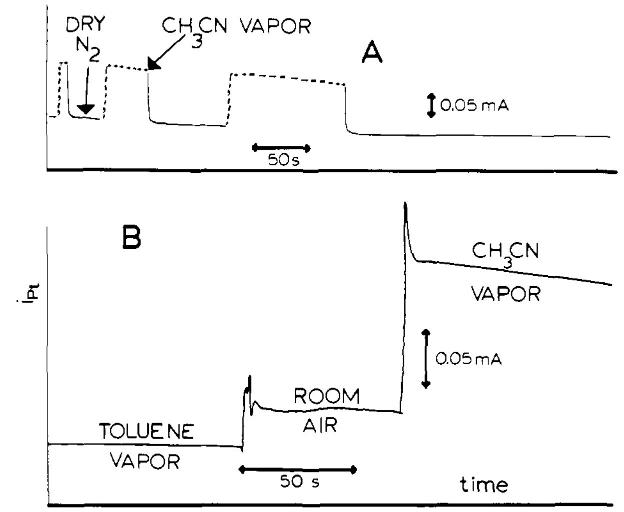

Figure 4. Case I, 1:1 Os(III/II) films prepolarized at ΔE giving limiting current $i_{L,3/2}$ and changed between indicated bathing gases. Curve A electrode is $\Gamma_T = 3.0 \times 10^{-8}$ mol/cm^2 and $\Delta E = 0.51$ V. Noise in Curve B results from manual handling of electrode during transfer.

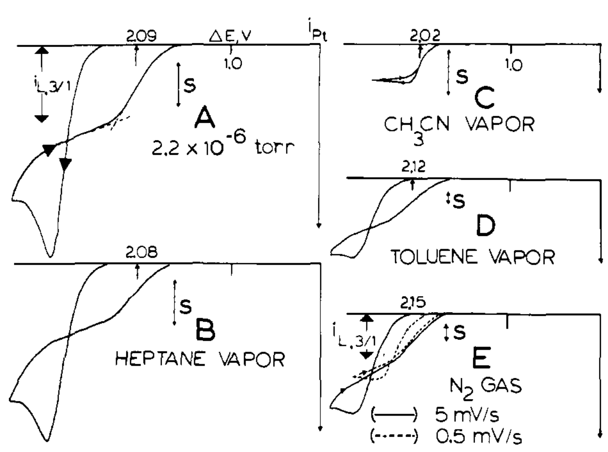

Figure 5. Case II voltammograms for the disproportionation of Pt/poly[Os(II)(bpy)$_2$(vpy)$_2$](ClO$_4$)$_2$/Au sandwiches in indicated bathing gases and at 5 mV/s except for curve E (---). Coverages are 3.2×10^{-8} (A–C), 2.0×10^{-8} (D), and 0.97×10^{-8} mol/cm^2 (E). Dashed lines in curve A represent how $i_{L,3/1}$ is measured on the decreasing ΔE scan.

on account of more positive site interaction activity terms,[23] in vapor than in liquid.

An informative, but qualitative, comparison between acetonitrile vapor and liquid can be based on how the voltammetry responds to the ΔE sweep rate. In liquid electrolyte, it is known[13,14] that at sufficiently high potential sweep rates, cyclic voltammetric responses become dependent on the rate of electron diffusion and the rate of counterion migration (or both). We have found that voltammograms of Pt/poly[Os(bpy)$_2$(vpy)$_2$](ClO$_4$)$_2$/Au sandwiches obtained by sweeping the Pt electrode potential vs. SSCE in liquid Et$_4$NClO$_4$/CH$_3$CN (holding the Au at 0 V) are typically relatively undistorted up to ca. 100 mV/s. In acetonitrile vapor, on the other hand, significant distortion and hysteresis is seen in the voltammetry of Pt/poly[Os(III/II)(bpy)$_2$(vpy)$_2$](ClO$_4$)$_{2.5}$/Au sandwiches at 100-mV/s sweep rates. The hysteresis between currents in increasing and decreasing ΔE scans is illustrated in Figure 3B; it becomes more pronounced when ΔE is swept more rapidly, and vanishes at very low sweep rates. Since we have learned from the limiting currents (vide supra) that *electron* mobilities, $D^l_{e,3/2}$ and $D^g_{e,3/2}$, are the *same* in acetonitrile liquid and vapor, the hysteresis must instead arise from the rate at which ClO$_4^-$ *counterions* can migrate across the film as the distribution of poly[Os(II)] and poly[Os(III)] sites is changed. The conclusion is that the ClO$_4^-$ ion is less mobile in vapor than liquid-bathed films.

In summary, our comparison of $D^l_{e,3/2}$ and $D^g_{e,3/2}$ between acetonitrile liquid and vapor shows that the dynamics of electron self-exchange between poly[Os(II)] and poly[Os(III)] sites are essentially identical in the two environments. This implies that a polymer film exposed to CH$_3$CN vapor can adsorb sufficient acetonitrile vapor to yield an internal solvation state similar to that occurring when the film is contacted by liquid acetonitrile. On the other hand, specific details like enhanced wave broadening and slowed ClO$_4^-$ mobility show that, while similar, the internal solvation states are not entirely identical in acetonitrile liquid and vapor.

When Pt/poly[Os(III/II)(bpy)$_2$(vpy)$_2$](ClO$_4$)$_{2.5}$/Au sandwiches are exposed to less polar bathing gases, the voltammetry resembles that of Figure 3, but the currents are smaller. The effect is reversible, as illustrated by Figure 4A where an electrode, with a ΔE impressed so as to give a limiting current $i_{L,3/2}$, was sequentially exposed to dry N$_2$ and acetonitrile vapor. The amount of residual CH$_3$CN retained by the film upon change to dry N$_2$ bathing gas is uncertain. Current thermogravimetry experiments and the immediacy of the changes in current seen in Figure 4A, however, show that most of the internal CH$_3$CN is rapidly removed in dry N$_2$. In Figure 4B, a series of bathing gases was used. This is also a sensitive way to confirm differences between several bathing gases, of values of $D^g_{e,3/2}$ (Table I), and of the corresponding poly[Os(II)]/poly[Os(III)] electron self-exchange rates. As was the case in acetonitrile, $D_{e,3/2}$ in toluene vapor (0.25×10^{-8} cm^2/s) is nearly the same as in liquid toluene (0.35×10^{-8} cm^2/s). By implication, $D^g_{e,3/2}$ in N$_2$ gas (0.4×10^{-8} cm^2/s) might thus be the same as "$D^l_{e,3/2}$" in a comparable liquid N$_2$ medium, if such an experiment were possible at room temperature.

Unsuccessful attempts were made to determine the electron diffusion coefficients $D^g_{e,2/1}$ and $D^g_{e,1/0}$ by electrolytically preparing the appropriate mixed-valent films and transferring them to various bathing gases. These experiments were plagued by the instability of the poly[Os(I)] and poly[Os(0)] films and the difficulty of maintaining an exact 1:1 mixed-valent situation. We consequently determined $D^g_{e,2/1}$ and $D^g_{e,1/0}$ (Table I) through the analysis and interpretation of the more complex case II and III voltammetries, considered next.

Case II. Electron Diffusion Driven by Disproportionation of Poly[Os(II)(bpy)$_2$(vpy)$_2$](ClO$_4$)$_2$/Au Sandwiches in Various Bathing Media. Voltammograms driving the disproportionation of Pt/poly[Os(II)(bpy)$_2$(vpy)$_2$](ClO$_4$) sandwiches in several bathing media are shown in Figure 5. Acetonitrile again affords the simplest comparison between bathing vapor and liquid behavior. In liquid acetonitrile/electrolyte, the average separation between the formal potentials of the poly[Os(III/II)] and poly-[Os(II/I)] couples is 2.06 V (Table II, "calcd $\Delta E'$"). In acetonitrile vapor, current–ΔE voltammograms (Figure 5C) of the same sandwiches gave the experimentally identical value of 2.05 V (Table II, "exptl $\Delta E_{1/2}$"). The correspondence of potentials confirms that the electrochemical reaction in the vapor-bathed experiment is oxidation of poly[Os(II)] sites at the positive (Pt) electrode to poly[Os(III)], reduction of poly[Os(II)] sites at the negative (Au) electrode to poly[Os(I)], and conproportionation of poly[Os(III)] and poly[Os(I)] in between, as depicted for case II in Figure 1.

Limiting currents of voltammograms in acetonitrile vapor (Table II, "exptl $i_{L,3/1}$") were analyzed in two ways. *Method i.* Assuming that D_e is the same in acetonitrile liquid and vapor, values of $D^l_{e,3/2}$ and $D^l_{e,2/1}$, determined in liquid electrolyte for each electrode, were used in eq 2 to calculate the $i_{L,3/1}$ expected for each electrode. These values (Table II, "calcd $i_{L,3/1}$") are nearly identical with (ratio 0.9) the experimental $i_{L,3/1}$ results. *Method ii.* Alternatively, using eq 2, $D^g_{e,2/1}$ was calculated from experimental $i_{L,3/1}$ values, using the average $D^g_{e,3/2} = 0.9 \times 10^{-8}$ cm^2/s of Table I. This comparison is more sensitive to experimental uncertainties, but the average $D^g_{e,2/1} = 14 \times 10^{-8}$ cm^2/s in Table II (right-hand column) is at best only slightly larger than $D^l_{e,2/1} = 6 \times 10^{-8}$ cm^2/s. That is, the electron self-exchange between poly[Os(II)] and poly[Os(I)] sites is the same or only slightly

---

(23) Chidsey, C. E. D.; Murray, R. W. *J. Phys. Chem.* **1986**, *90*, 1479.

Table II. Determination of $D^{g}_{e,2/1}$ and $\Delta E_{1/2}$ from Case II Disproportionation of Poly$[Os(bpy)_2(vpy)_2]^{2+}$ Films

bathing medium/ counterion^a	$\Gamma_T \times 10^8$,^{b} mol/cm^2	$i_{L,3/1}$, A/cm^2		$\Delta E_{1/2}$, V		$D^{l}_{e,3/2} \times$ 10^8,^{e} cm^2/s	$D^{l}_{e,2/1} \times$ 10,^{e} cm^2/s	$D^{g}_{e,2/1} \times$ 10^8,^{f} cm^2/s
		exptl	calcd^c	exptl	calcd^d			
CH_3CN vapor/ClO_4^-	0.69	1.59	1.62	2.1		1.6	7.9	18.2
	0.74	1.44	1.59	2.09	2.08	1.9	6.4	17.1
	1.41	0.61	0.47	2.06	2.04	1.0	4.1	10.0
	1.53	0.29	0.57	2.05	2.05	1.2	6.1	1.41
	1.66	0.48	0.49	2.09	2.06	1.4	4.3	8.1
	2.36	0.28	0.30	2.04	2.05	1.0	4.8	5.1
	2.54	0.47	0.47	2.05	2.05	1.6	9.5	23.1
	2.72	0.22	0.34	2.04	2.06	1.4	6.0	3.42
	3.22	0.17	0.17	2.02	2.06	0.8	4.4	3.13
av		0.9 ± 0.2	exptl/calcd	2.05 ± 0.03	2.06 ± 0.01	1.2 ± 0.5^g	6 ± 2^g	14 ± 8^g
CH_3CN vapor/Tos^-	2.28	0.17	0.07	2.08	2.01	0.08	0.28	
	2.54	0.17	0.07	2.05	2.04	0.10	0.23	
	3.79	0.07	0.16	2.08	2.08	0.26	1.42	
av		1.8	exptl/calcd	2.04 ± 0.03	2.04 ± 0.02	0.15 ± 0.05	0.64 ± 0.4	

[a] Medium is N_2 saturated with acetonitrile vapor at room temperature. The counterion is exchanged into the film from an acetonitrile solution, followed by rinsing and air drying in the poly[Os(II)] state. [b] Quantity of electroactive Os complex sites in sandwiches as determined cyclic voltammetrically. [c] Calculated from eq 2 using the $D^{l}_{e,3/2}$ and $D^{l}_{e,2/1}$ values determined for each electrode, assuming that $D^{l}_{e,3/2} = D^{g}_{e,3/2}$ and $D^{l}_{e,2/1} = D^{g}_{e,2/1}$. [d] Difference between $E^{\circ\prime}(3/2)$ and $E^{\circ\prime}(2/1)$ determined in 0.1 M Et_4NClO_4/CH_3CN or 0.1 M Et_4NTos/CH_3CN. [e] Determined by sandwich electrode voltammetry in 0.1 M Et_4NClO_4/CH_3CN or 0.1 M Et_4Tos/CH_3CN. [f] Calculated from eq 2 using the average $D^{g}_{e,3/2}$ values (found in Table I), measured in CH_3CN vapor (for the CH_3CN vapor/ClO_4^- case) with the respective individual $i_{L,3/1}$ experimental values. [g] Average includes determinations taken in Table III. Also listed in Table I.

accelerated in the vapor-bathed film.

Analogous comparisons were made between acetonitrile vapor and liquid for Pt/poly$[Os(II)(bpy)_2(vpy)_2](Tos)_2$/Au sandwiches into which the tosylate anion had been incorporated. Since $D^{g}_{e,3/2}$ is not available for tosylate films, the liquid/vapor comparison was made as in method i above. While the data are more limited, Table II shows that the experimental and calculated $i_{L,3/1}$ currents are not very different (ratio 1.8), and $\Delta E_{1/2}$ is the same.

$\Delta E_{1/2}$ and $i_{L,3/1}$ from voltammograms recorded in other bathing media (Figure 5) are summarized in Table III. The inclusion in these results of voltammograms recorded at 10^{-6} torr vacuum is noteworthy, since observations on *functioning* electrochemical cells in vacuo are quite rare. In most cases, disproportionation voltammograms were recorded both in acetonitrile vapor and the alternative bathing gas, to improve the accuracy of defining the environmental effects.

The solid-state voltammetric half-wave potentials, ($\Delta E_{1/2}$, Table III) are in the correct range for the expected 2Os(II) → Os(III) + Os(I) disproportionation, but $\Delta E_{1/2}$ in the less polar media are consistently larger than in acetonitrile (120 to 190 mV in toluene vapor and electrolyteless liquid toluene, respectively, and 50–70 mV in dry N_2, vacuum, and heptane vapor). These effects may in part be ohmic (*iR*) losses from residual potential gradients in the film, but can also represent thermodynamic destabilization of poly[Os(III)] or poly[Os(I)] states (or both) relative to poly-[Os(II)]. That poly[Os(III)] sites should be destabilized in less well ionically solvating media is an expectable result.

Examination of the Figure 5 voltammograms shows substantial hysteresis in the nonpolar media as compared to acetonitrile vapor. Apparent but clearly nonequilibrium current plateaus occur in both the increasing and decreasing ΔE scans. Slowing the ΔE scan rate greatly lessens the hysteresis, as demonstrated in Figure 5E, which also shows that in a voltammogram with hysteresis, the $i_{L,3/1}$ observed during the *decreasing* ΔE scan is more nearly equal to the equilibrium value. Values of $i_{L,3/1}$ in Table III were measured in this way. Note that the existence of the hysteresis, as discussed above, qualitatively means that the migration of the ClO_4 counterions to form the case II concentration gradients occurs more slowly when very nonpolar bathing media are employed.

The most striking result in Table III is that limiting currents $i_{L,3/1}$ for disproportionation of Pt/poly$[Os(II)(bpy)_2(vpy)_2]$-$(ClO_4)_2$/Au sandwiches in toluene and heptane vapor, N_2 gas, and 10^{-6} torr vacuum are consistently *larger* than those in acetonitrile vapor. This important effect was confirmed by experiments like Figure 6, top, where ΔE was applied to a sandwich in acetonitrile vapor so as to produce an equilibrated $i_{L,3/1}$ limiting current, and then the bathing gas was changed to dry N_2 (- - -) and back to acetonitrile vapor. Values of $D^{g}_{e,2/1}$ in the nonpolar media were calculated (Table III) as in method ii above. The average results are collected in Table I. We see that the rates of self-exchange between poly[Os(II)] and poly[Os(I)] sites in films bathed by toluene vapor or dry N_2 are *ca. 10× faster than in acetonitrile vapor.* From the similarity of the $i_{L,3/1}$ limiting currents in vacuo and heptane vapor to those in N_2 bathing gas (Table III), we can surmise that $D^{g}_{e,2/1}$ is also larger in those media. In sharp contrast, $D_{e,2/1}$ in pure toluene *liquid* is *smaller* by ca. 300×, than $D_{e,2/1}$ in toluene vapor.

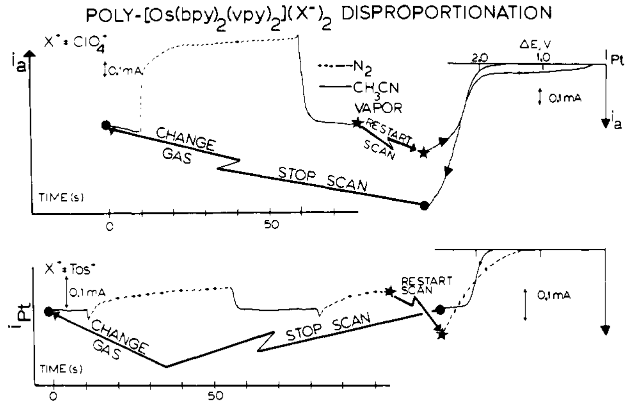

Figure 6. Poly$[Os(II)(bpy)_2(vpy)_2](X)_2$ case II disproportionation currents, $i_{L,3/1}$, depend on bathing gas. In each case, the film first is polarized with a ΔE giving $i_{L,3/1}$ in acetonitrile vapor (—) (2.8 V in ClO_4^- and 2.5 V in Tos^-), and then switched to a dry N_2 bathing gas (- - -): $\Gamma_T = 2.2 \times 10^{-8}$ mol/cm^2.

Significant additional results were obtained from Pt/poly-$[Os(II)(bpy)_2(vpy)_2](Tos)_2$/Au films containing tosylate anions. These films give no observable voltammetry when ΔE is scanned in a dry N_2 bathing gas, which means that the tosylate anion mobility is so low in the dried films that its *long-range* (distance of many monolayers) migration, necessary to form concentration polarized films, cannot be seen on reasonable timescales. That is, electron mobility is quenched by lack of long-range counterion mobility. On the other hand, voltammograms can be observed in acetonitrile vapor (Figure 6, bottom), where apparently tosylate mobility is much greater. If in acetonitrile vapor ΔE is now scanned to a potential to allow concentration polarization to be established and the $i_{L,3/1}$ limiting current to flow, and the bathing gas changed to N_2, the effect of a N_2 bathing gas on electron exchange can now be observed free from tosylate mobility restrictions. The necessary long-range tosylate migration has already

Table III. Case II: Effects of Bathing Medium on $D^{g}_{e,2/1}$ and Potentials $\Delta E_{1/2}$ for Poly[Os(bpy)$_2$(vpy)$_2$](ClO$_4$)$_2$ Disproportionation

	$i_{L,3/1}$,[a] A/cm^2						$\Delta E_{1/2}$,[a] V						$D^{g}_{e,2/1} \times 10^8$,[b] cm^2/s			
$\Gamma_T \times 10^8$, cm^2/s	CH$_3$CN vapor	tol vapor	tol liq	dry N$_2$	10^{-6} vac	hept vapor	CH$_3$CN vapor	tol vapor	tol liq	dry N$_2$	10^{-6} vac	hept vapor	CH$_3$CN vapor	tol vapor	tol liq[c]	dry N$_2$[d]
1.54			0.21						2.28						0.47	
1.55			0.15						2.15						0.10	
1.80			0.22						2.27						0.95	
2.00	0.50	0.65		0.65				2.12		2.09			14.9	132		46, 139
1.74	0.57	0.86		0.76				2.12		2.11			14.3	176		63, 118
1.95	0.62	0.78		0.82				2.18		2.11			23.2	180		76, 225
1.95	0.52	0.76		0.62				2.28		2.09			14.9	172		40, 124
2.87	0.38	0.52		0.52				2.10		2.06			16.9	170		55, 154
6.84	0.18			0.21			2.02						24.9			51, 142
7.62	0.17			0.23			2.01						29.0			87, 234
1.66	0.48			1.22	1.19	0.90	2.09			2.09	2.10	2.15	8.1			123, 335
1.41	0.58			1.02	1.27	0.92	2.06			2.08	2.14	2.10	9.0			57, 158
3.22	0.17			0.41	0.37	0.24	2.02			2.09	2.09	2.08	3.1			45, 127
						av	2.04 ± 0.03	2.16 ± 0.07	2.23 ± 0.06	2.09 ± 0.02	2.11 ± 0.03	2.11 ± 0.03	15.8 ± 8.1	166 ± 19	0.5 ± 0.4	120 ± 47

[a] Measured from the current plateau on the decreasing ΔE scan. [b] Calculated from eq 2 using the average $D^{g}_{e,3/2}$, for each gas, together with the experimental $i_{L,3/1}$ values, except for toluene liquid, where D_e is for a liquid ($D^{l}_{e,2/1}$) and $D^{l}_{e,3/2} = 0.35 \times 10^{-8}$ cm^2/s was employed for the calculation. [c] Pure toluene liquid, no electrolyte added. [d] Calculated individually from the two $D^{g}_{e,3/2}$ results in N$_2$ (Table I) to emphasize the sensitivity in eq 2 to $i_{L,3/1}$ and $D^{g}_{e,3/2}$ and the consequent uncertainty range in $D^{g}_{e,2/1}$.

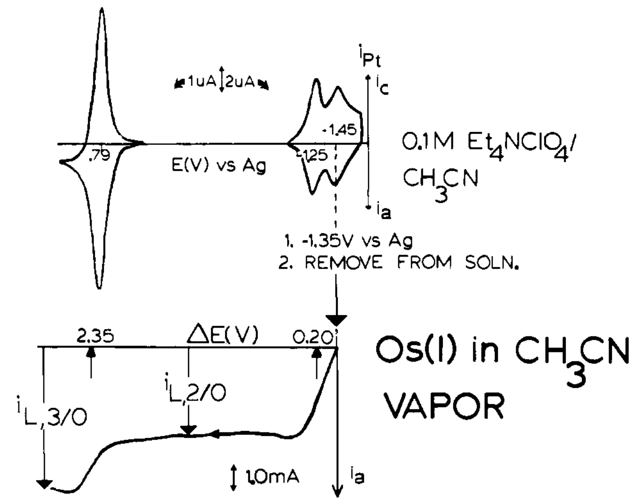

Figure 7. Case III disproportionation of a Pt/poly[Os(I)(bpy)$_2$(vpy)$_2$](ClO$_4$)/Au sandwich prepared by electrolysis at the potential indicated on the cyclic voltammogram (upper curve), followed by transfer to acetonitrile vapor and scan of ΔE (lower curve): 10 mV/s and Γ_T = 7.6 × 10^{-8} mol/cm^2.

occurred while in the acetonitrile bathing gas. Figure 6 (bottom) shows the effects of switching between the two bathing gases for such a prepolarized sandwich. Just as in the case of ClO$_4^-$ films, $i_{L,3/1}$ is *larger* in the dry N$_2$ bathing gas. We infer that electron self-exchange between poly[Os(II)] and poly[Os(I)] sites is accelerated in a dried film, in spite of the low mobility of the tosylate counterion. It follows that *the electron hopping event involves little if any counterion displacement in the poly[Os(II/I)] reaction.*

Cases II and III. Electron Diffusion Driven by Disproportionation of Pt/Poly[Os(I)(bpy)$_2$(vpy)$_2$](ClO$_4$)/Au Sandwiches in Acetonitrile Vapor. The poly[Os(I)] sandwiches were prepared by electrolyzing a poly[Os(II)] film at a potential more negative than $E^{\circ\prime}$ for Os(II/I) in Et$_4$NClO$_4$/CH$_3$CN, disconnecting the electrode, removing it from the solution, rinsing with pure acetonitrile, and drying in the Ar glovebox atmosphere. Solid-state voltammetry in acetonitrile vapor is illustrated in Figure 7, with data given in Table IV. Two waves are observed, the first being for the case II disproportionation reaction 2Os(I) → Os(II) + Os(0) and the second wave for the case III double disproportionation reaction 3Os(I) → 2Os(III) + Os(0). There are good matches between the expected and experimental $\Delta E_{1/2}$ (Table IV).

Following method ii above, values of $D^{g}_{e,2/1}$ were employed with the case II $i_{L,2/0}$ limiting currents and eq 2 to evaluate $D^{g}_{e,1/0}$. $D^{g}_{e,1/0}$ is also evaluated from case III $i_{L,3/0}$ limiting current (at ΔE = 2.75 V) with eq 5 using $D^{g}_{e,3/2}$ and $D^{g}_{e,2/1}$. The uncertainty in these calculations was large, both because the $i_{L,3/0}$ currents were not very stable and because of the sensitivity of $D^{g}_{e,1/0}$ to the chosen values of $D^{g}_{e,3/2}$ and $D^{g}_{e,2/1}$. However, the average $D^{g}_{e,1/0}$ = 149 × 10^{-8} cm^2/s (Table I) is similar to that seen in acetonitrile liquid, 96 × 10^{-8} cm^2/s.

In connection with the double disproportionation reaction, it is interesting that the concentration gradient profile of the redox couple with the smallest electron diffusion coefficient ($D^{g}_{e,3/2}$) becomes compressed over a quite small interval of the overall film thickness. In Figure 7, we estimate that when $i_{L,3/0}$ is flowing, the poly[Os(III/II)] couple occupies only $^1/_{19}$th of the overall film thickness, or about 40 layers of sites over this interval. Recalling that applying Fick's laws to the electron self-exchange process involves the basic assumption of *medium continuity* (by stating the electron motion as a diffusion problem), the shrunken poly[Os(III/II)] profile raises an interesting and fundamental possibility. If our sandwich-making technology could be improved to attain an overall film dimension of 1.9 × 10^{-9} mol/cm^2, instead of the present ca. 7 × 10^{-9} mol/cm^2 lower limit, the poly[Os(III/II)] "profile" would be only *one monolayer* of sites thick. Clearly continuity would be violated in such a circumstance, and the Fickian formulation should fail.

Table IV. Case III: Double Disproportionation of Poly[Os(I)(bpy)$_2$(vpy)$_2$](ClO$_4$) Films in Acetonitrile Vapor

$\Gamma_T \times 10^8$, mol/cm^2	$i_{L,2/0}$, A/cm^2	$\Delta E_{1/2,2/0}$, V		$D^{g}_{e,1/0} \times 10^8$,[b] cm^2/s	$i_{L,3/0}$, A/cm^2	$\Delta E_{1/2,3/0}$, V		$D^{g}_{e,1/0} \times 10^8$,[c] cm^2/s
		exptl	calcd[a]			exptl	calcd[a]	
7.31	5.8	0.19	0.21	160	9.5	2.40	2.22	488
6.84	2.65	0.11	0.21	11	4.8	2.22		71
7.62	3.2	0.20	0.21	32	5.4	2.35		133
				av 68				231

[a] Evaluated from differences between $E°'(2/1)$ and $E°'(1/0)$ (for $\Delta E_{1/2,2/0}$) and $E°'(3/2)$ and $E°'(1/0)$ (for $\Delta E_{1/2,3/0}$). [b] Calculated from eq 4, for $i_{L,2/0}$, and average $D^{g}_{e,2/1}$ of Table I. [c] Calculated from eq 5, for $i_{L,3/0}$, and average $D^{g}_{e,3/2}$ and $D^{g}_{e,2/1}$ of Table I.

Conclusions

Two sets of general conclusions can be drawn from the above results. Firstly, eq 1–5 as formulated in cases I–III appear to quantitatively represent the electrochemical reactivity of redox polymers that have a resident pool of mobile counterions and transport electrons by concentration gradient-driven hopping, like Pt/poly[Os(bpy)$_2$(vpy)$_2$](X)$_n$/Au sandwich films. This is most definitely established by the acetonitrile vapor experiments and gives us confidence to use the theory to evaluate $D^{g}_{e,2/1}$ values in unusual, gaseous bathing media like toluene vapor and dry N$_2$. The behaviors of these thus determined electron diffusion coefficients reflect changes in electron self-exchange rate constants as we manipulate the state of solvation of the exchanging centers. We conclude that the sandwich electrode experiment (or its lithographically defined array electrode equivalent[15]) provides a powerful entree to solid-state electron transfer chemistry. The requirement for applying the approach is, of course, that the material of interest is both an electron and an ion conductor on a reasonable timescale.

The second general conclusion is that the values of the electron self-exchange rate constants of the poly[Os(III/II)] and poly[Os(I/II)] couples in these films, as embodied in $D^{g}_{e,3/2}$ and $D^{g}_{e,2/1}$, respectively, are strongly affected by the nature of the bathing medium. Furthermore, they *can respond differently to certain media*, as seen in Table I. *$D^{g}_{e,3/2}$ decreases* in N$_2$ and in toluene vapor,[24] which most likely reflects additional barriers to electron transfer imposed by loss of polymer microfluidity or local counterion mobility in the dried film. One might then expect, simplistically, that drying the film should depress the rates of all the other electron self-exchange processes as well. This seems indeed to occur for poly[Os(II/I)] self-exchange in toluene liquid; $D^{l}_{e,3/2}$ and $D^{l}_{e,2/1}$ are both smaller than the corresponding values in acetonitrile vapor and liquid.

Consequently, the finding that, although $D^{g}_{e,3/2}$ decreased upon transfer of bathing environment from acetonitrile to dry N$_2$ or toluene vapor, $D^{g}_{e,2/1}$ *increased* instead was quite unexpected. These would appear to be two alternative interpretations of this result. The first is that, upon drying in N$_2$, the microfluidity of the polymer (and thus the ease of crossing barriers associated with counterion motion and polymer chain motions) increases when the polymer is in a poly[Os(II/I)] mixed-valent but decreases in the poly[Os(III/II)] state. The second interpretation, and the one we favor, is that *the counterion or polymer motions that are associated with electron transfers from poly[Os(I)] to poly[Os(II)] sites are less pronounced than those involved in poly[Os(III/II)] self-exchange*. Central to this interpretation is the plausible supposition that the polymer site–site spacing will be somewhat smaller in a N$_2$-dried as compared to an acetonitrile-swollen film. This supposition is supported by a profilometry-based swelling measurement[25] showing that a poly[Os(II)] film increases ca. 8% in thickness when bathed in CH$_3$CN vapor. We think it is also important that poly[Os(II/I)] self-exchange involves mostly (bpy) ligand-centered orbitals whereas those involved in poly[Os(III/II)] self-exchange are more metal centered. Consequently, achieving the poly[Os(II/I)] transition state in a dry film may require little or no polymer backbone or counterion motion (recall Figure 6B), being between already closely spaced bpy/bpy$^{\bullet-}$ moieties, whereas achieving the poly[Os(III/II)] transition state requires more pronounced motions. Put differently, the site–site separation dependency of poly[Os(II/I)] self-exchange rates is stronger than those of poly[Os(III/II)] self-exchange.

With respect to the decrease of $D^{g}_{e,3/2}$ in dry N$_2$, we should remark that we have recently measured electron transport in poly[Os(bpy)$_2$(vpy)$_2$](ClO$_4$)$_{2.5}$ films over a –90 to +50 °C temperature range. The essential finding of this study, described elsewhere,[26] is that the *electron transport follows the same Arrhenius relation (constant activation barrier) over this entire temperature range*. Given that the lower temperatures are below T_{fp} of CH$_3$CN, and give exceedingly low ClO$_4^-$ mobilities, it seems likely then that the barrier to poly[Os(III/II)] self-exchange originates from some internal polymer motion. The result also provides no support for a tunneling mode of electron transfer.

Finally, we should remark upon the absolute value of $D^{g}_{e,2/1}$ in N$_2$ and in toluene vapor, which is by far the largest electron diffusion coefficient encountered for a redox polymer. According to theory by Saveant and Laviron,[14] values of D_e are proportional to electron self-exchange rate constants by the relation

$$D_e = 10^3 k_{ex,app} C_T (\Delta X)^2 \tag{6}$$

where ΔX is the average site–site distance in the polymer. Values of C_T = 1.5 M and ΔX = 1.4 nm in eq 6 give $k_{ex,app} = 0.6 \times 10^8$ M^{-1} s^{-1} for $D^{g}_{e,2/1} = 1.7 \times 10^{-6}$ cm^2/s. This value is a lower limit since ΔX in the transition state of a bpy/bpy$^{\bullet-}$ reaction is undoubtedly smaller than the 1.4-nm metal–metal spacing.

Acknowledgment. This research was supported in part by a grant from the Office of Naval Research. The authors acknowledge helpful discussions and reprint of ref 16b from Professor R. P. Buck (UNC).

---

(24) An experiment like Figure 4A was not done for dry N$_2$ vs. toluene vapor, and their $D^{g}_{e,3/2}$ values in Table I should not be regarded as experimentally distinguishable.

(25) A poly[Os(II)]X$_2$ film was deposited on a SnO$_2$ electrode and exposed to an CH$_3$CN vapor bath while the profilometer stylus was tracking over the polymer surface. A thickness increase of ca. 8% was observed.

(26) Jernigan, J. C.; Murray, R. W. *J. Phys. Chem.*, submitted.